Optical Description of Microscopic Surface Structure of Photographic and Ink Jet Prints

Osamu Ide

Research & Development Center, Document Products and Supply Company, Fuji Xerox Co., Ltd., Kanagawa-ken, Japan

To prepare photographic quality prints, an optimization of surface structure of the print is very important. Conventionally, the structure has been evaluated in terms of the geometric profile obtained with a surface roughness-measuring device. However, the geometric profile does not directly reflect the appearance of the print surface. Therefore, by simulating the unconscious visual operation, a microscopic surface analyzing method has been devised: a print surface was illuminated with a light flux transmitting through a slit, and the distribution of surface reflected light was captured by an area sensor placed in the specular direction. Evaluation of various print surfaces by this method proved that the surface can be characterized in terms of the following two indices; the average width and the gravity variation of the reflected image. This optical analysis correlates well with the subjective texture of print surface.

Journal of Imaging Science and Technology 47: 447-454 (2003)

Introduction

Recently, with the advent of marking technologies that have remarkably improved image quality, along with the prevalence of digital still cameras, many hardcopy output devices that are designed to provide photographic quality prints have been launched into the market. Among the quality attributes of photographic quality prints, not only the conventional four primary ones, i.e., color and tone reproduction, graininess, and sharpness, but also the surface property or texture of the print is very important.[1] In order to achieve photographic quality by means of an output device not based on the silver halide technology, the print surface structure must be designed suitably.

Now let me recapitulate the main proposals on print surface property control in the thermal dye transfer segment. FUJIX VP-6000, a video graphic printer introduced into the market in 1989 by Fuji Photo Film, was optionally equipped with a small laminator called Fine Finisher, through which the print was passed with a piece of PET film superimposed thereon. The heating roller pressed the smooth surface of the PET film against the print surface to make it as smooth as the film. Then, in the XL 8600 printer from Eastman Kodak in 1993, a full-color print was first formed with four thermal ribbons, and thereafter uniformly covered with a transparent resin layer from a resin-coated ribbon, thus achieving a markedly improved print surface smoothness. MJ-2000 printer of Alps Electric Co., based on thermal polymer transfer, followed the above described technique of uniform coating of a transparent layer using a waxy material, in order to simulate the appearance of the photographic print surface.

In the case of ink jet printing wherein most of the colorant is absorbed into the medium, the print surface structure is strongly dependent on that of the printing medium. Accordingly, a number of media for photographic quality prints are sold in the market.

In electrophotography, one can use a medium having a surface resembling that of the photographic print as in ink jet printing. Although the non-image area of the print retains the surface property of the medium itself, the image area consists of a relatively bulky toner layer that protrudes from the medium surface. Hence, the print surface consists of raised image areas against almost smooth non-image areas. A countermeasure for this problem has been reported in which a layer of transparent colorless toner is further transferred onto the color-image bearing medium to achieve high gloss, independent of image density.[2] As another method, e.g., in Pixography of Xerox Corp., color toner images are transferred onto a medium having a surface layer made of a thermoplastic resin. In the following thermal fixing process, the color toners are embedded into the resin layer, thus giving a print with uniform surface gloss.

For the design of preferable print surfaces, it is essential to quantitatively analyze the differences in the surface structure of prints. The present paper discusses methods for such analysis.

Conventional Surface Structure Analyses

Conventionally, the surface structure of print has been described by surface glossiness or the angular variation

Original manuscript received April 8, 2003

Tel: 81-465-80-2387, Fax: 81-465-81-8964;
E-mail: ide.osamu@fujixerox.co.jp

of the light reflected from the print. It should be noted that these two descriptors represent print characteristics averaged over broad areas of print. However, when a human observer examines a highly glossy surface such as that of a glossy photographic print, this observer's preference is governed by the microscopic structure including slight undulations, minute concavity and convexity present in the print surface. Accordingly, for the present purpose, a new method is necessary that can quantitatively describe such microscopic structure of print surface.

As a method of microscopic surface analysis, fine surface tracing by means of a surface roughness meter is well known. This method suffers from the difficulty in correlating the result thus obtained with how the surface appears for the observer. Since the print observer judges the surface quality mainly optically, an optical method capable of describing the microscopic characteristics of the print surface seems preferable.

Optical Evaluation of Microscopic Surface Characteristics

First of all, the procedure of surface structure evaluation by the observer is considered. The diffusely reflected light from a print is supplementary to the colorant absorption; in contrast, the surface reflected light, free of the influence of absorption, substantially retains the spectral property of the illuminant. The color of the reflected light, which is the sum of these two kinds of light, changes depending on the macroscopic surface structure.

Now, a highly glossy surface containing mild undulations is assumed. The surface reflected light distributes around the specular direction. In the case where a microscopic unevenness exists in the surface, the light scattered by the unevenness is expanded substantially uniformly over a wide range of angle to impart a hazy or cloudy impression to the print. But, if the number of convexities as well as concavities is relatively small in the illuminated region, then the intensity of the scattered light impinging into human eye will be negligible. Thus, the difference in surface structure among glossy prints is hardly detectable in terms of color difference under a standard colorimetric condition such as 0/45.

Actually, under such measuring condition, no difference in color reproduction characteristics has been observed between two high gloss prints, one being a silver halide photographic print having weak undulations, and the other being the same photographic print laminated with an extremely flat transparent film.

However, a surprisingly clear difference is observed between the two surfaces when the observer looks at the reflected image of a light source such as a fluorescent lamp placed in the specular direction relative to the observer's eye. On the surface of the photographic print, he can recognize the contour but not the detail of the fluorescent lamp. On the other hand, on the film-laminated print, he recognizes the detail of the lamp and distortion of the lamp image contour. We infer that human observers utilize such a difference among glossy surfaces for the judgment of the print surface quality. Therefore, an analytical method that correlates well with surface appearance will be derived by simulating this phenomenon.

The above procedure is elucidated optically. Suppose a glossy surface is illuminated with a collimated light flux. If a small fractional area in the surface is inclined by θ from its average direction, the reflected light deviates by 2θ. Thus, the angular fluctuation in reflected light is twice as much as that in the surface. It is concluded that by illuminating a print surface with a collimated light flux transmitted through a slit, and capturing the reflected light through the slit by means of an image capture device placed in the specular direction, one can detect the angular fluctuation of light and thus describe slight differences in microscopic surface structure. A correspondally similar method is already in use for the evaluation of paint-coated surfaces. In the method, a periodically intensity-modulated light pattern is projected on a paint-coated flat surface, and the image clarity value is defined as the ratio of intensity modulation of the reflected light from the surface to that from a reference surface.[3]

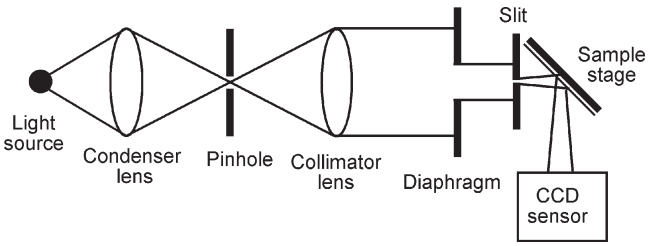

Figure 1. Schematics of the measuring apparatus.

Measuring Apparatus

The measuring apparatus designed according to the concept described above is schematically shown in Fig. 1. In this apparatus, a collimated light flux is directed to a slit and the light that is transmitted by the slit illuminates the surface of a print. A two-dimensional image capture device arranged in the specular direction measures the intensity distribution of the surface reflected light. The light source was a halogen lamp while the image capture device was a CCD camera (Mega Plus 4.2 of Kodak, with $2{,}029 \times 2{,}044$ pixels, each pixel being of 9×9 μm size). Since the angular variation is not considered to be strongly dependent on the direction of incidence in the present measurement, this direction was fixed to 45 degrees relative to the surface. To minimize noise, image capture was performed at a shutter speed of 500 ms and a gain of –6db. The infrared component was cut off by a filter.

Resolution-Determining Factors

In Fig. 1, we assume a perfectly collimated light, and neglect the diffraction at the narrrow slit. Then, the specularly reflected light from an optically flat surface projects on the CCD a very fine, sharp line representing the slit aperture. With an actual print surface containing microscopic undulations, part of the reflected light deviates from the specular direction. Thus, the system resolution is determined by the angular detectivity of the CCD, i.e., the angle corresponding to the unit pixel of the CCD. Since the above assumptions do not hold in our actual system, discussion is necessary on the degree of collimation and the diffraction at the slit.

Degree of Collimation

The degree of collimation is determined by the diameter of the pinhole and the focal length of the collimator lens. The former, which governs the light intensity at the print surface, was set at 0.2 mm to secure measuring efficiency, while the latter was 200 mm. Then, the

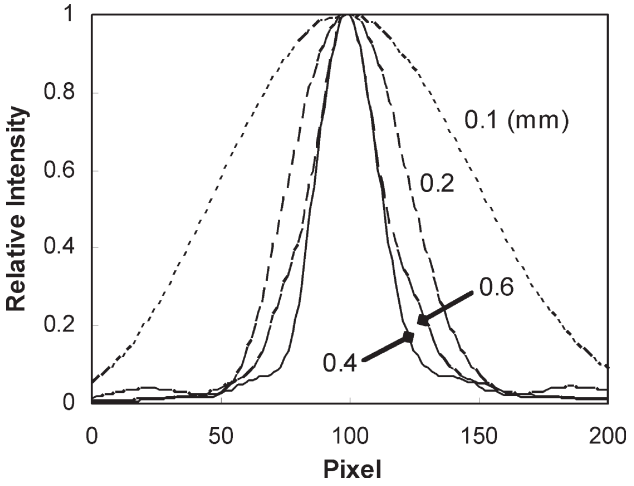

Figure 2. Intensity distributions of the light reflected from an optically flat surface with various slit widths.

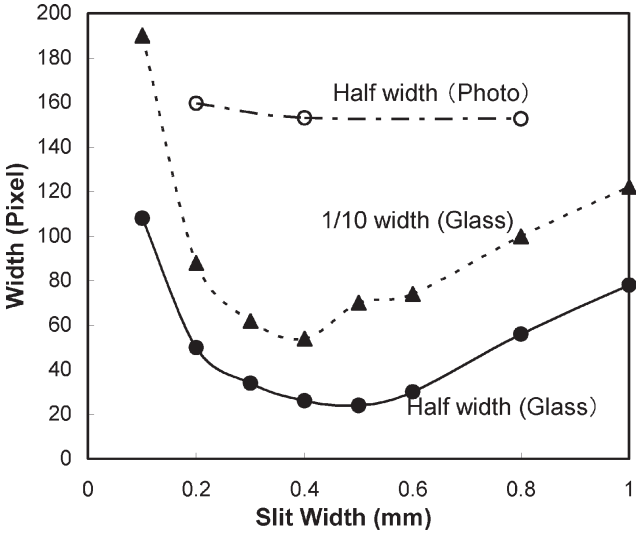

Figure 3. Dependence of the half and one-tenth widths of reflected light intensity distributions on slit width.

degree of collimation is equal to $\pm 0.5 \times 10^{-3}$ rad (0.003°). This value has substantially no influence on the overall system resolution as confirmed by calculation below.

Diffraction at the Slit

It may look promising for the analysis of fine structures to make the illuminated area small with use of a narrow slit. However, a narrow slit is accompanied by a spread due to Fresnel diffraction, which expands the illuminated area on the print. Since diffraction deteriorates the degree of collimation, the light reflected by the print further expands towards the CCD.

The degree of diffraction spread on the CCD can be reduced by making the distance from the slit to the CCD small whereby, however, the spread of the reflected light due to the undulation in the print surface, which is the signal to be detected, is also reduced. In other words, the S/N wherein noise is associated with the diffracted light is substantially independent of the slit-to-CCD distance. Hence, this distance is determined from the viewpoint of angular detectivity to be described shortly. To minimize the influence of diffraction at the print surface, in our experiments the slit was arranged as close as 15 mm to the surface to prevent mechanical interference. The optimal slit width must be determined experimentally.

Angular Detectivity of CCD

This factor depends on the distance between the print surface and the CCD, and the CCD resolution. This distance was fixed at 165 mm so that the signal component reflected from the print surface does not exceed the CCD area. Since the distance from the print surface to the CCD is 165 mm and the pixel size is 9×9 μm, the angular detectivity is 5.45×10^{-5} rad (0.00313°).

Slit Width Optimization

By changing the width of a 10 mm long, variable width slit (07SLT001, a product of Melles Griot), we measured the intensity distribution of the light specularly reflected at the optically flat surface of a standard glass plate for gloss measurement (a product of Murakami Color Research Laboratory). Figure 2 contains one-dimensional intensity distributions obtained by averaging the two-dimensional data over the slit length. The intensities plotted along the ordinate are normalized by the peak value for each slit width. Figure 3 shows the dependence on slit width of half and one-tenth widths of light intensity distribution, and further the half widths corresponding to a silver halide photographic print. From these two figures, it is evident that, with use of an optimal slit width of 0.4 to 0.5 mm, the resulting system resolution is high enough for the surface analysis on photographic-like prints.

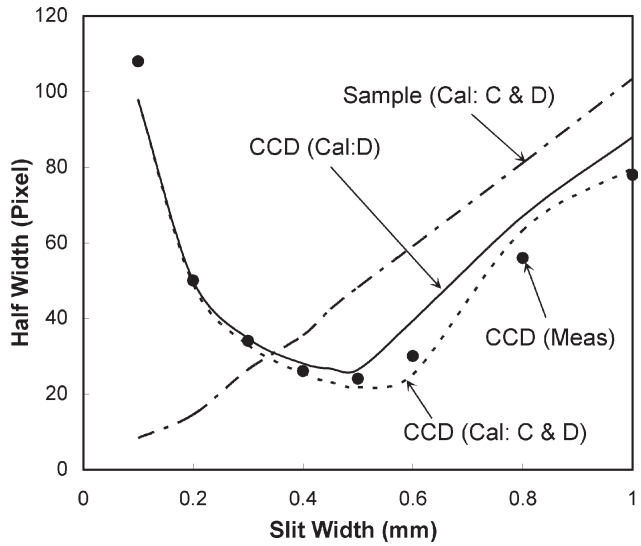

Figure 4. Dependence of the calculated (Cal) and measured (Meas) half widths of reflected light intensity distributions at the sensor plane and sample plane on slit width. C: Collimation (ϕ = 0.2 mm, f = 200 mm), D: Diffraction

We now confirm by calculation whether the results obtained above are reasonable. Figure 4 shows the spread by the slit in terms of half width at a wavelength of 550 nm calculated by the Fresnel-Kirchhoff diffraction formula.[4] In addition to the calculated curve with the actual collimation, the figure also includes experi-

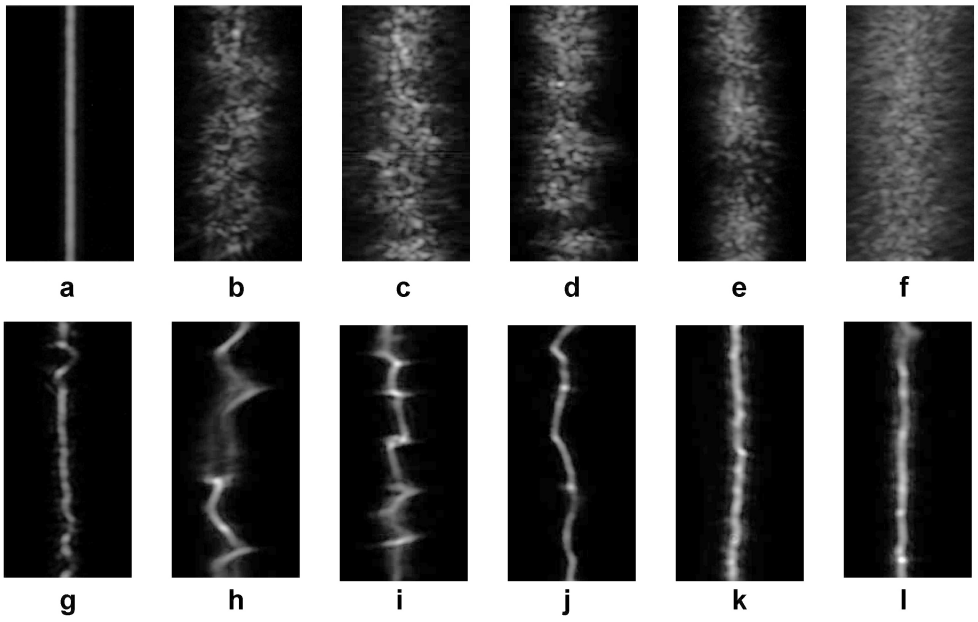

Figure 5. Reflected light distributions captured by the CCD area sensor (256 × 512 pixels). a: Standard glass, b: Silver halide photograph, c: Pictrography® print, d: PM/PP, e: BJF/PP, f: PM/Film, g: BJF/Film, h: Pictrography print (L), i: PM/PP(L), j: BJF/PP(L), k: PM/Film(L), l: BJF/Film(L), (PM: PM-3300, BJF: BJF850, /PP: Photographic® Paper Base Substrate, /Film: Film Base Substrate, (L): with Lamination)

mentally measured values. The calculated values coincide well with the measured ones. These data indicate that spread on the CCD is mainly governed by slit diffraction, and that the effect of collimation level is far weaker. Figure 4 also includes the half width of the illuminated light on the print plane: the spread on the print plane is nearly proportional to the slit width.

In order to satisfy the two purposes, i.e., minimization of the illuminated area on the print and suppression of the spread at the CCD due to slit diffraction, a slit width of 0.4 mm was judged most desirable within the optimal range cited above.

Evaluated Print Samples

As the print samples to be evaluated, silver halide photographic prints and ink jet prints were prepared. To minimize the effect of diffuse reflection, solid black areas were measured.

A silver halide monochromatic print was prepared on glossy photographic paper, Fujibro WP FM3 of Fuji Photo Film Co., Ltd. Another print was made with Pictrography® 3000 (a product of Fuji Photo Film Co., Ltd.) based on a photothermographic transfer process. Ink jet prints were prepared with PM-3300 of Seiko Epson Corporation and BJF-850 of Canon Inc. with use of a glossy film-based medium and a photo paper medium both designed for exclusive use of each system. Further, each print was laminated with a transparent film by means of a laminator developed for Pictrography®.

Results and Discussion

Comparison of the Reflected Light Profile

Figure 5 shows the two-dimensional distributions of the reflected light intensity for the various print surfaces, captured with the CCD camera. In the figure, the distributions designated as g, k and l are very close to that of the standard optical glass (a), being almost straight with narrow widths. Those designated as h, i and j are undulated to a considerable extent with narrow widths. Further, those designated as b, c, d, e and f exhibit broad widths. At the same time, it is likely that the intensity variations along the slit direction are different from print to print.

The width of the distribution is interpreted as representing the surface roughness component owing to microscopic unevenness present in the reflection surface, while the degree of straightness of the distribution is interpreted as representing the undulation component owing to low spatial frequency undulation in the surface.

Descriptors for Reflected Light Profile

Now, the distribution thus observed must be characterized by appropriate metrics. An x-axis was defined as the direction corresponding to the slit width, and a y-axis as the direction corresponding to the slit length. As the metric corresponding to the width of the distribution, the average half width W was assumed; W was derived by averaging the half width values for all y coordinates. Further, as the metric for the half width variation, the standard deviation of the half width values was adopted.

As for the metric corresponding to the straightness of the distribution, the center of gravity $G(y)$ along the x-axis direction at each y value was calculated, and standard deviation of $G(y)$ was taken as a metric. If we imagine how the variation of $G(y)$ appears to observers, then, it will be understood that low spatial frequency components are more readily detected visually. Accordingly, the variation of $G(y)$ was subjected to spatial frequency analysis, the resulting spectrum was multiplied with by the visual transfer function representing the frequency response characteristics of human vision.[5] By integrating the multiplied values, the Wiener Spectrum, WS value for the variation of $G(y)$ was obtained as another metric. A metric for the reflection intensity varia-

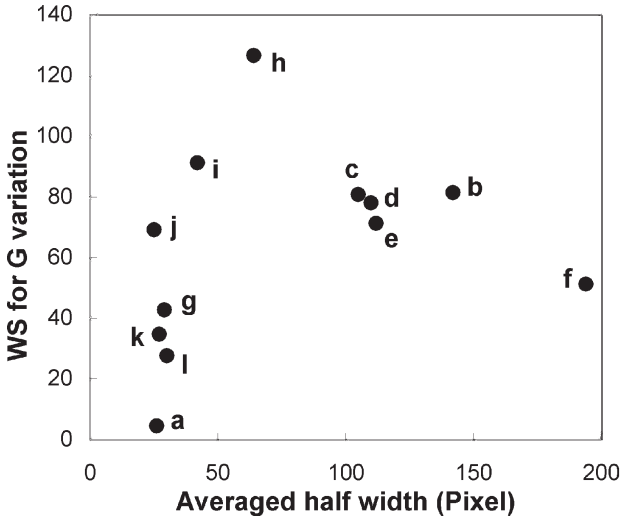

Figure 6. Surface characteristics plotted in the plane for the two metrics.

tion was defined by the standard deviation of the reflection intensity peak Rp at each y-coordinate.

The correlation between the average half width W and the half width variation was very high with the r^2 value not less than 0.9. The correlation between the standard deviation of $G(y)$ and the WS value for the variation of $G(y)$ was similarly high. Also, the standard deviation of $G(y)$ correlates with the standard deviation of Rp with an r^2 value around 0.65. From these relationships, we find that the print surface property can be characterized by only two metrics, one being the average half width W (or the half width variation), and the other being the WS for the variation of $G(y)$ (or the standard deviation of $G(y)$.

In Fig. 6, surface characteristics are plotted on the plane between the average half width W and the WS for the variation of $G(y)$. From the figure, it is evident that the Pictrography® quality print and the ink jet print using a photographic quality paper achieved similar surface characteristics to those of the silver halide photographic quality print. When these prints are laminated with the film, the WS increases although the half width reduces. The print surface prepared by ink jet with film substrates followed by film lamination is close to the standard glass surface, thus located near the origin of the coordinates.

Comparison with Human Vision

To achieve a close correlation with print appearance, it is desirable to compare quantitatively the present measuring system with the human visual system. In my measuring system, the surface illumination reaches the surface of the image capture plane directly without passing through any focusing optics. On the other hand, in the visual system, the reflected light is focused on the retina through an optical system including the cornea and lens. The differences between the two systems may be analyzed as follows.

Deviations in the Measuring System

When a minute area inclined relatively to the average sample plane by $\alpha/2$, the light reflected by this area advances in the direction inclined by α relative to the average reflection angle. In the measuring system where the distance from the sample to the image capture plane is L, and where the effects of the degree of collimation and diffraction at the slit are assumed negligibly small compared to α. Then, the deviation on the image capture plane h corresponding to the angular deviation α is;

$$h = L\alpha. \tag{1}$$

The angular resolution of the experimental system, which is determined mainly by slit diffraction, is calculated to be 0.03 degrees.

Deviations in the Human Visual System

As was mentioned above, when one perceives undulations or unevenness present in a highly glossy surface, such perception or judgment comes from the blur as well as the distortion of the illuminant such as a fluorescent lamp projected on the surface. Under such conditions, the visual system is considered to focus on the light source so that the image of the light source is focused on the retina. Figure 7 schematically shows the visual system during surface property examination. When the angle of inclination of the reflected light is small, the image height H' on the retina is given by the following Eq. (2).

$$H' = \alpha \cdot A \cdot D/n \cdot (A + B), \tag{2}$$

in which A represents the distance from the light source to the sample plane, B that from the sample plane to the visual optics, i.e., viewing distance, D that from the visual optics to the retina, i.e., eyeball diameter, and n the refractive index inside the eyeball, respectively. The figure reveals that the light beam impinging onto a point inclined by $+\alpha/2$ appears as if emitted from a point displayed by H from the light source, where H is given by,

$$H = \alpha \cdot A. \tag{3}$$

From Eq. (2), the deviation H' on the retina is proportional to the angular deviation α just as the deviation h in the measuring system. However, H' depends on both the source-sample distance, A, and the viewing distance, B. How H' changes with A and B is shown in Fig. 8. H' increases monotonically with A. Hence, the farther the light source is placed from the sample plane, the detectivity for angular deviations in the sample increases. Accordingly, the angular resolution of the visual system is substantially unaffected by the slit diffraction which was an issue in the measuring system, but depends significantly on the aberration of the optics.

In the design of a measuring apparatus simulating the visual system, it is necessary to take into consideration the dependence of the angular fluctuation on the two distances (the source-to-sample distance and the sample-to-optical system distance). The aberration of the optics then determines the angular resolution of such measuring apparatus.

Magnification and Focal Length of the Visual System

The visual optics alters its focal length depending on the distance to an object to be viewed, whereby the magnification also changes. Let m' be the magnification of the visual optics when the light source is focused, then the following relation holds;

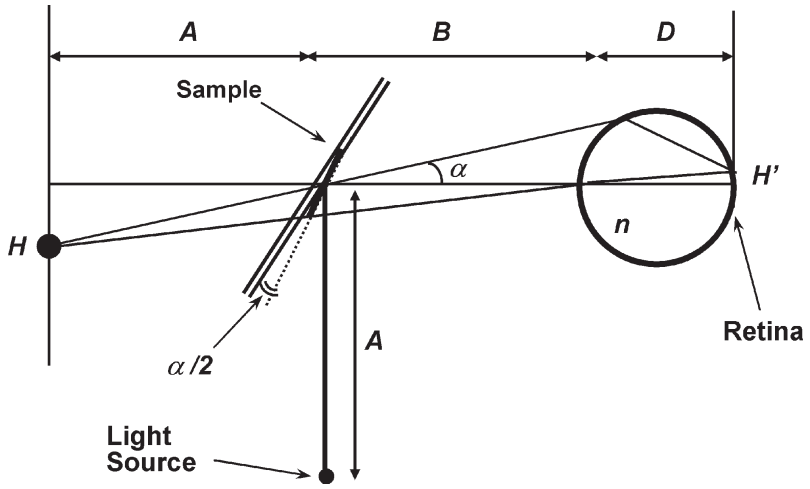

Figure 7. Schematic of the visual system.

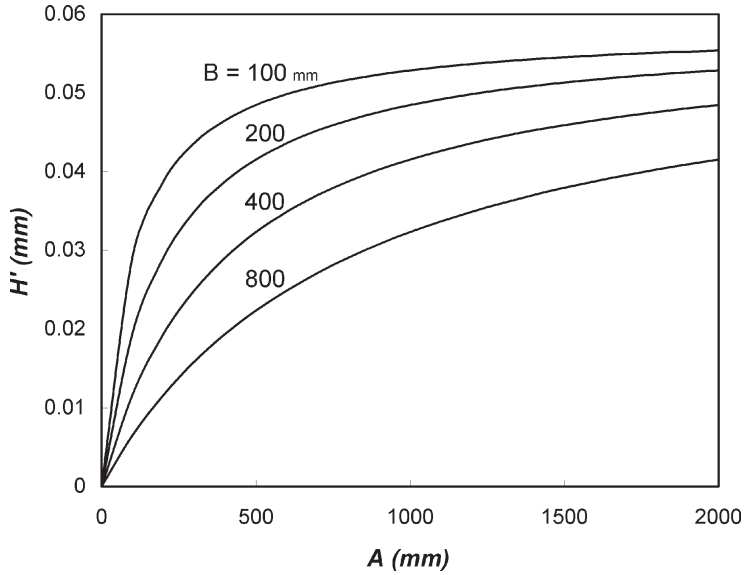

Figure 8. Dependence of the deviation at the retina on A and B. $\alpha = 0.2°$, $D = 22.22$ mm, and $n = 1.333$

$$m' = D/n \cdot (A + B). \quad (4)$$

If the focal length on the object side is defined as f', then f' is expressed as

$$f' = (A + B) \cdot D/\{n \cdot (A + B) + D\}. \quad (5)$$

On the other hand, for m, which is the magnification of the visual optics for the condition of focusing on the sample plane, then

$$m = D/n \cdot B. \quad (6)$$

If one defines the focal length in the object side as f, then

$$f = B \cdot D/(n \cdot B + D). \quad (7)$$

Optical Parameters of the Eye

An optical system simulating the eye is called a "schematic eye", and there are many papers dealing with the schematic eye.[6-8] Here, the optical parameters for the reduced eye devised by Listing will be used for discussion.

The changes in the focal lengths f' and f due to the change of viewing distance are shown in Fig. 9. The object side focal length of the visual optics is 16.67 mm for infinitely long viewing distance and 15.79 mm for a standard viewing distance of 300 mm. The difference between these two focal lengths is only 5%. Such a small difference comes from the fact that the viewing distance of 300 mm is about 20 times as large as the focal length. Further, the larger the light source-to-sample distance becomes, the less the contribution of the viewing distance B on f' becomes. The pupil aperture under print viewing conditions is around 4 to 5 mm while the f-number is about 3.5.

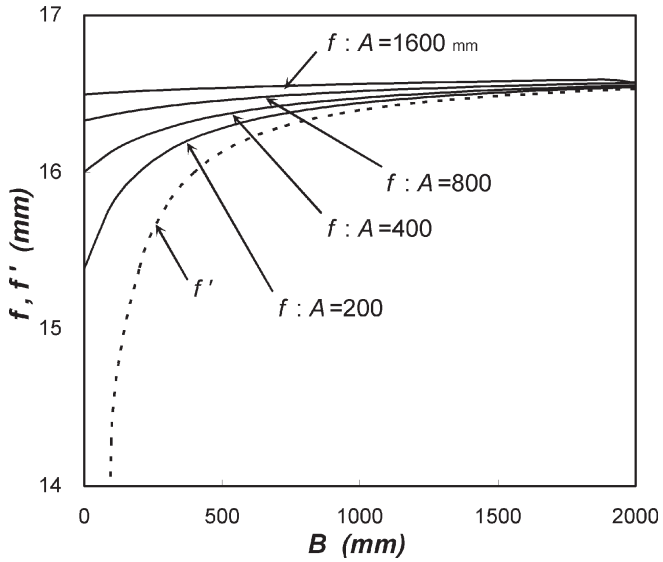

Figure 9. Dependence of the focal length of the visual system on A and B. D = 22.22 mm, and n = 1.333

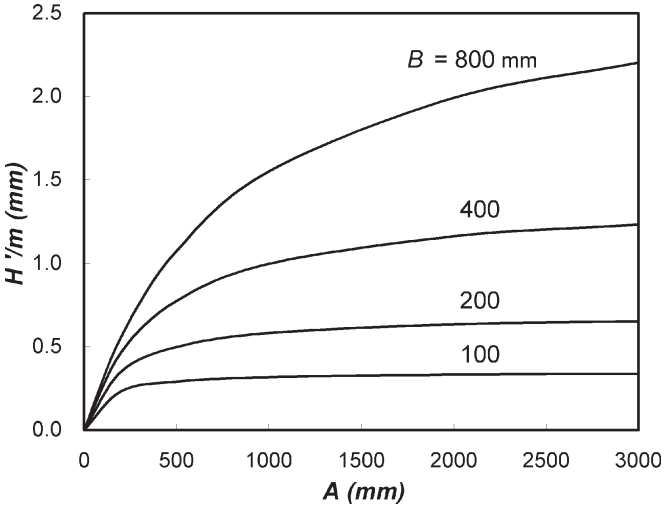

Figure 10. H'/m dependence on A and B. $\alpha = 0.2^{\circ}$.

Appearance of Angular Variation

How the reflected image of a light source in the surface of a glossy print appears for various combinations of A and B was next investigated. For a constant B, the degree of blur and distortion appeared to increase for larger A's. Likewise for a constant A, the degree of blur and distortion appeared to increase for larger B's.

Normalization Measure in the Visual System

Figure 8 suggests that, if the observer perceives the degree of angular variation in terms of the absolute value for H', then the detectivity will be enhanced when A is long with short B. However, this assumption does not agree with the subjective impression mentioned in the preceding section. This disagreement indicates that the dimensional judgment of an image focused on the retina is not based on the absolute height of the image, but a certain height relative to some normalization measure. It is tentatively assumed, as a very simplified model, that the normalization measure is a dimension in a single plane. Then, such plane must be chosen from two candidates, i.e., the light source plane and the sample plane. Firstly, the light source plane is chosen wherein the degree of blur and distortion width used for perception are absolute shifts in the light source plane. The perceived dimension is expressed by

$$H'/m' = \alpha \cdot A. \tag{8}$$

Hence, if the light source is located at infinity, then the variation of the reflected image must be perceived to be infinitely large. Moreover, the observer should not recognize the variation of the reflected image of a knife edge, for which the dimension and the distance do not make any sense. These conclusions conflict with the subjective experience of viewing surface reflection images.

Therefore, assuming that the observer normalizes the variation of reflection images with the dimension in the sample plane. Then, the height to be perceived is given by

$$H'/m = \alpha \cdot A \cdot B/(A + B). \tag{9}$$

The changes in H'/m due to the changes in A and B are shown in Fig. 10. The qualitative trend of these changes agrees with the subjective experience described in the previous section.

These facts suggest that, in the perception of the surface structure of a print sample, the human observer relies on the degree of relative variation normalized by a dimension on the sample, not on the absolute variation in the reflection image formed on the retina.

Actual print viewing will be often made with a viewing distance B of 300 mm, and the distance to the light source A of about 2000 mm, whereby the value of H'/m does not dramatically depend on either A or B. Accordingly, the cited viewing condition is regarded appropriate for the subjective evaluation of print surface structure.

Elucidation of the Measuring System

In the foregoing section, I proposed as the indices for the description of print surface structure, the average half-width of the reflected light distribution for the slit that describes the degree of blur, and the WS for G variation that describes the degree of distortion. It should be noted that the latter index has been derived by taking into account not only the amplitude but also the spatial frequency characteristics of the reflected image based on the spatial response of human vision.

While the amplitude, i.e., the amount of light scattering in the slit width direction is proportional to A, the proportionality constant varies with the geometrical arrangement of the measuring system. But, if the conditions are fixed, both the half-width and the distortion amplitude are multiplied by the same proportionality constant. The spatial frequency characteristics of the distortion are associated with the sample surface itself. In the present measuring system, the slit length is captured in its actual size; thus, the appropriate frequency response function is the one corresponding to the viewing distance adopted in the subjective evaluation, i.e., 300 mm.

In the investigation of the correlation between the subjective surface structure and the above cited indices, the contribution of the proportionality constants can be ignored within the range of linear analysis.

However, since such constants vary as to the degree of contribution in non-linear analyses, proportionality constants must be transformed appropriately so as to reflect the viewing conditions. This situation holds also to the measuring system which simulates the human visual system.

Comparison of Angular Resolution

One may adopt an imaging optical system analogous to the human eye whereby optical parameters for the eye may be chosen for the system. Alternatively, the system may be designed with optical parameters appropriate for measurement by taking into consideration the sensor size and the system magnification. The measured values may then be converted by calculation to those which the observer perceives.

For example, in the case where an image is captured in actual size at the distance of 300 mm, then the use of a macro lens of 150 mm focal length will be needed. Generally speaking, such a lens has a resolution limit of about 20 μm. Thus, if an apparatus incorporating an imaging optical system is built, the resolution will be enhanced by at least one order of magnitude compared to the diffraction limited value. However, the present measuring apparatus is provided with sufficient resolution for detection of the angular fluctuation in the image plane of the media of interest.

Conclusions

I have succeeded in detecting the microscopic surface structure of photographic quality prints by illuminating the print surface with the light flux diffracted at a slit on which a collimated light flux was illuminated, and measuring the intensity distribution of the reflected light by means of a CCD area sensor placed in the specular direction.

The intensity distribution could be classified in terms of two metrics representing the width and straightness of the distribution, i.e., the average half width and the variation of the center of gravity. The coordinates on the plane for the above two descriptors are considered to correlate well with the subjective texture of print surface. Furthermore, by taking into consideration the optical parameters of the visual system and the standard viewing distance, it is possible to estimate how the above cited intensity distribution is perceived by the observer.

In the near future, I will further investigate preferable print surface characteristics through subjective evaluation to confirm the degree of correlation of print surface preference with the above metrics for the design of print surface characteristics. In cases where more delicate differences among highly smooth surfaces are to be detected, an apparatus design based on imaging optics simulating the human visual system must be investigated. ▲

Acknowledgment. The author expresses his thanks to Dr. Sizuo Tatuoka and Dr. S. Honjo for their comments.

References

1. S. Honjo, On Photography, *J. Imaging Soc. Japan* **39**, 66 (2000).
2. O. Ide & M.Kurimoto, Image Quality Improvement with Surface Structure Modification in Xerography, *J. Imaging Soc. Japan* **38**, 103 (1999).
3. ASTM Designation: D 5767, Standard Test Methods for Instrumental Measurement of Distinctness-of-Image Gloss of Coating Surface, (Reapproved 1999).
4. M. Born and E. Wolf, *Principles of Optics* 3rd ed., Pergamon Press, Oxford, 1965, 380.
5. R. P. Dooley and R. Shaw, Noise Perception in Electro-photography, *Appl. Photogr. Eng.* **5**, 190 (1979).
6. H. Uosato, Optics Specific to Human Eye (In Japanese), *O plus E*, **22**, 418 (2000).
7. Y. Le Grand, *Form and Space Vision*, Indiana Univ. Press, Bloomington, 1967.
8. H. H. Emsley, *Visual Optics*, Hatton Press, London, 1936.